FEBS Letters

FEBS PRESS science publishing by scientists

Transient receptor potential V4 channel stimulation induces reversible epithelial cell permeability in MDCK cell monolayers

Minagi Mukaiyama[1], Yohei Yamasaki[1], Takeo Usui[2,3] and Yoko Nagumo[2,4]

1 Graduate School of Life and Environmental Sciences, University of Tsukuba, Japan
2 Faculty of Life and Environmental Sciences, University of Tsukuba, Japan
3 Microbiology Research Center for Sustainability (MiCS), University of Tsukuba, Japan
4 Alliance for Research on the Mediterranean and North Africa (ARENA), University of Tsukuba, Japan

Correspondence
T. Usui and Y. Nagumo, Faculty of Life and Environmental Sciences, University of Tsukuba, Tsukuba, Ibaraki 305-8572, Japan
Tel: +81 29 853 6629
E-mails: usui.takeo.kb@u.tsukuba.ac.jp (TU); nagumo.yoko.fn@u.tsukuba.ac.jp (YN)

(Received 3 April 2019, revised 3 June 2019, accepted 3 June 2019, available online 26 June 2019)

doi:10.1002/1873-3468.13490

Edited by Maurice Montal

The transient receptor potential V4 channel (TRPV4) is responsive to a variety of physical and chemical stimuli, including a synthetic agonist GSK1016790A (GSK). Here, we show that TRPV4 is functionally expressed in, and that GSK induces the reversible opening of tight junctions (TJs) in epithelial Madin–Darby canine kidney II monolayers. Stimulation of TRPV4 by GSK induces an increase in fluorescein isothiocyanate-conjugated dextran (4 kDa) permeability and a reduction in transepithelial resistance, and these responses are blocked by pretreatment with the specific TRPV4 antagonist. Small conductance, but not large conductance Ca^{2+}-activated K^+ channels, TRPA1 channel, and cofilin activation are involved in TRPV4-mediated reversible opening of TJs. These results suggest that a novel mechanism underlies TRPV4-mediated regulation of the tightness of epithelial barriers.

Keywords: capsaicin; cofilin; epithelial permeability; tight junction; TRPA1; TRPV4

Transient receptor potential V4 channel (TRPV4) is a nonselective cation channel with a moderate preference for Ca^{2+}. TRPV4 exhibits a polymodal gating and is responsive to a large variety of physical and chemical stimuli, including moderate heat, hypotonicity-induced cell swelling, flow, endogenous ligands, and synthetic agonists, such as GSK1016790A (GSK) [1]. TRPV4 has been found in both excitable and nonexcitable cells in many different tissues, where it regulates diverse cellular functions. For instance, TRPV4 has been shown to regulate the barrier function of endothelial [2,3], and epithelial cells [4–10]. In skin keratinocytes, TRPV4 activation is important for tight junction (TJ) establishment and also strengthens TJ barrier function [4,5,8]. Interestingly, it has also been reported that TRPV4 activation leads to increased paracellular permeability or decreased transepithelial electrical resistance (TER) in mammary and intestinal epithelial cell lines [7,10], although our study here shows the different patterns of epithelial permeability increase and the mode of actions.

We have been interested in the regulation of TJ permeability and have analyzed the capsaicin-induced reversible increase in paracellular permeability [11–16]. Recently, we reported that capsaicin and natural compounds containing an α,β-unsaturated moiety open

Abbreviations
4α-PDD, 4α-phorbol 12,13-didecanoate; A96, A-967079; AITC, allyl isothiocyanate; BK channels, large conductance Ca^{2+}-activated K^+ channels; FD4, fluorescein isothiocyanate-conjugated dextran (4 kDa); GSK, GSK1016790A; HBSS, Hank's Balanced Salt Solution; HC, HC-067047; HRP, horseradish peroxidase; LatA, latrunculin A; MDCK, Madin–Darby canine kidney; RuRed, ruthenium red; SK channels, small conductance Ca^{2+}-activated K^+ channels; TER, transepithelial electrical resistance; TJ, tight junction; TRP, transient receptor potential.

TJs reversibly *via* TRPA1 activation, but not by TRPV1 activation [17] in monolayers of the canine kidney epithelial cell line Madin–Darby canine kidney (MDCK) II, although capsaicin is an agonist of the TRPV1 cation channel.

Here, we functionally characterize TRPV4 in MDCK II epithelial cells. TRPV4 mRNA expression was confirmed, and its activation a specific agonist, GSK, resulted in rapid Ca^{2+} influx. Treatment of the MDCK II monolayer with GSK induced a reversible increase in fluorescein isothiocyanate-conjugated dextran (4 kDa; FD4) permeability and a reversible decrease of TER. These responses were blocked by pretreatment with a specific TRPV4 antagonist, HC-067047 (HC) [18], suggesting that TRPV4 activation is involved in TJ opening. Ca^{2+} entry through TRPA1 and cofilin activation are involved in capsaicin-induced reversible opening of TJs. Although Ca^{2+} entry *via* GSK triggers an immediate decrease in TER and an increase in FD4 permeability, cofilin activation did not occur at all. Our data show that TRPV4 stimulation induces an increase in reversible paracellular permeability in MDCK II monolayers by a different mechanism from TRPA1 activation.

Materials and methods

Cell culture and reagents

Madin–Darby canine kidney II cells were cultured in Dulbecco's Modified Eagle's Medium (Nacalai Tesque, Kyoto, Japan) supplemented with 10% fetal bovine serum (HyClone, GE Healthcare, Buckinghamshire, UK) and 1% penicillin–streptomycin (Nacalai Tesque) in a humidified atmosphere containing 5% CO_2.

GSK, HC, paxilline, and A-967079 were from Cayman (Ann Arbor, MI, USA). Capsaicin and FD4 were purchased from Sigma (St. Louis, MO, USA). Latrunculin A (LatA) and ruthenium red (RuRed) were from Wako Pure Chemical Industries (Osaka, Japan). Ionomycin and allyl isothiocyanate (AITC) were purchased from LKT Laboratories (St. Paul, MN, USA) and Tokyo Chemical Industry Co., Ltd. (Tokyo, Japan) respectively.

Anti-cofilin antibody (#3312) was purchased from Cell Signaling Technology (Beverly, MA, USA). Anti-β-actin (#125K4769) and anti-claudin-2 (#SAB4503544), anti-phospho-cofilin (Ser 3, #sc-21867-R), anti-claudin-1 (#13050-1-AP), and anti-TRPV4 (#ab94868) antibodies were from Sigma, Santa Cruz Biotechnology (Santa Cruz, CA, USA), Proteintech Group, Inc. (Rosemont, IL, USA), and Abcam (Cambrigde, UK) respectively. Anti-occludin (#71-1500) and anti-claudin-4 (#329400) antibodies were from Invitrogen (Grand Island, NY, USA). Horseradish peroxidase (HRP)-conjugated anti-mouse and anti-rabbit IgGs (#5220-0341 and #5220-0336, respectively) were from Kirkegaard & Perry Laboratories (Gaithersburg, MD, USA).

All other reagents were of reagent grade and purchased from Nacalai Tesque unless otherwise noted.

RNA preparation and PCR

RNA was isolated from a MDCK II monolayer established as described below using a NucleoSpin RNA II kit (Macherey-Nagel, Düren, Germany) according to the manufacturer's protocol. First-strand cDNA was synthesized using a PrimeScript II 1st strand cDNA synthesis kit (TAKARA, Kyoto, Japan). PCR was performed using KOD Dash (TOYOBO, Osaka, Japan) in a TAKARA PCR Thermal Cycler Dice® Gradient with specific primer sets as follows: GAPDH, 5′-GAAAGCTGCCAAATAT GACGACATC-3′ (forward) and 5′-TCCAGGAGGCTCT TACTCCTTG-3′ (reverse); TRPV4, 5′-GGACGAGGT GAACTGGTCTCACT-3′ (forward) and 5′-GGAGCATC GTCAGTCCTCCACT-3′ (reverse); and TRPA1, 5′-CTA CATGCATAATGTAGAGG-3′ (forward) and 5′-GGAG CAGATATTAATAGCAC-3′ (reverse). PCR condition was as follows: 1 cycle at 98 °C for 30 s, 30 cycles at 94 °C for 30 s, 55 °C for 20 s, and 74 °C for 30 s followed by 1 cycle at 74 °C for 4 min.

Cytotoxicity assay with MDCK II monolayer

Madin–Darby canine kidney II cells were seeded into a 96-well plate (Iwaki, Tokyo, Japan) at a density of 3.4×10^4 cells per well. The cells were cultured for 3 days to establish monolayer integrity and then treated with various concentrations of GSK. After 5 h, 10 μL of Cell Counting Kit-8 (Dojindo Laboratories, Kumamoto, Japan) reagent was added to each well. The plate was incubated at 37 °C, and absorbance at 450 nm was then measured using an iMark Microplate Reader (Bio-Rad Laboratories, Inc., Hercules, CA, USA) prior to calculation of IC_{50} values.

Intracellular Ca^{2+} measurements

Madin–Darby canine kidney II cells were seeded into 96-well plates with clear bottoms and black walls (Greiner Bio-One, Frickenhausen, Germany) at a density of 3.4×10^4 cells per well. The cells were cultured for 3 days, with the medium being changed every day to establish monolayer integrity. After experimental treatment, monolayers were washed with Hank's Balanced Salt Solution (HBSS; 136.9 mM NaCl, 5.4 mM KCl, 1.3 mM $CaCl_2$, 0.8 mM $MgSO_4$, 0.34 mM Na_2HPO_4, 0.44 mM KH_2PO_4, 1.0 $g \cdot mL^{-1}$ glucose, and 4.2 mM $NaHCO_3$) and treated with Fluo-8 loading buffer [5 μM Fluo-8 (AAT Bioquest, Sunnyvale, CA, USA), 2.5 mM probenecid (Cosmo Bio,

Tokyo, Japan), and 1% F-127 (Biotium, Hayward, CA, USA) in HBSS] at 37 °C for 1 h. Cells were washed with HBSS twice, and recording buffer (2.5 mM probenecid in HBSS) and various compounds were then added. Fluo-8 fluorescence was measured every 3 min for 60 min using a PowerscanHT fluorescence microplate reader (Dainippon Sumitomo Pharma, Osaka, Japan) at excitation and emission wavelengths of 485 and 528 nm respectively.

Transport studies

Madin–Darby canine kidney II cells were seeded into 6.5-mm-diameter transwells (pore size 0.4 mm; Corning Inc., Corning, NY, USA) coated with collagen at a density of 3.4×10^4 cells per well. The cells were cultured for 3 days to establish monolayer integrity. Transwell plates were washed three times, incubated with HBSS, and equilibrated for 1 h at 37 °C. HBSS containing 1.0% w/v of FD4 was placed on the apical side, and transport enhancer was also added to the apical side. The basolateral side was exposed to HBSS, which was refreshed at predetermined intervals. Samples collected from the basolateral compartments were analyzed for FD4 using a PowerscanHT fluorescence microplate reader at an excitation wavelength of 485 nm and an emission wavelength of 530 nm.

Hank's Balanced Salt Solution lacking $CaCl_2$ was used in experiments with Ca^{2+}-depleted conditions.

TER measurements

Madin–Darby canine kidney II cells were seeded into 12-mm-diameter transwells (pore size 0.4 mm) coated with collagen at a density of 1.1×10^5 cells per well. The cells were cultured for 3 days to establish monolayer integrity. TER was measured as described previously [17].

Hank's Balanced Salt Solution lacking $CaCl_2$ was used in experiments with Ca^{2+}-depleted conditions, and TER was measured before and after adding drugs.

Localization of FD4 in cell layer

Madin–Darby canine kidney II monolayers grown on eight well coverglass chamber (Iwaki) were washed with HBSS, and incubated with HBSS for 1 h at 37 °C. The monolayers were treated with HBSS (0.2 mL) containing 1.0% w/v of FD4 and drugs for 30 min, with 2 $\mu g \cdot mL^{-1}$ Hoechst 33258 (Sigma) for the last 10 min, then washed three times with HBSS, and fluorescence images were acquired with a Leica DMI6000B microscope (Leica Microsystems, Heidelberg, Germany) within 20 min. The *z*-stacks were collected at 0.24 μm intervals. Image stacks were deconvoluted using LEICA APPLICATION SUITE X software (Leica Microsystems).

Immunoblotting

Madin–Darby canine kidney II cells were seeded into 24-well plates (Iwaki) at a density of 2.1×10^5 cells per well. The cells were cultured for 3 days, and the medium was changed every day to establish monolayer integrity. After specific treatments, monolayers were washed once with phosphate-buffered saline and lysed with SDS sample buffer (62.5 mM Tris-HCl, pH 6.8, 2% SDS, 10% glycerol, and 5% β-mercaptoethanol). After sonication, the cell extracts were boiled at 65 °C for 10 min, separated by sodium dodecyl sulfate-polyacrylamide gel electrophoresis, transferred to a polyvinylidene fluoride microporous membrane (Wako), blocked with 5% skimmed milk (Megmilk Snowbrand, Sapporo, Japan), probed with the appropriate primary and HRP-conjugated anti-IgG secondary antibodies, and visualized by enhanced chemiluminescence (Nacalai Tesque). Images were produced using a Sayaka Imager (DRC, Tokyo, Japan). Band intensities of phospho-cofilin and actin were measured with IMAGEJ software (NIH, Bethesda, MD, USA) and normalized to actin.

Data analysis

GRAPHPAD PRIZM 6, (GraphPad Software Inc., San Diego, CA, USA) was used to perform the analysis of variance for multiple comparisons. $P < 0.05$ was considered to be statistically significant.

Results

TRPV4 is functionally expressed in MDCK II monolayer

We previously demonstrated that TRPA1 is involved in the reversible opening of TJs in MDCK II epithelial monolayers [17]. Because TRPA1 is a TRP channel protein and TRPV4, the other TRP channel protein, is abundantly expressed in the kidney [19], we examined the mRNA expression of TRPV4 in MDCK II monolayers and detected TRPV4 at similar levels as TRPA1 (Fig. 1A). We also examined the expression of TRPV4 on the protein level by western blot analyses using an anti-TRPV4 antibody. Figure 1B shows the expression of a protein of ~ 90 kDa, which is in good agreement with the others reported [20,21].

To confirm functional TRPV4 expression in MDCK II monolayers, we examined cellular responses to the reported TRPV4 agonist GSK using Fluo-8, a fluorescent Ca^{2+}-imaging probe (Fig. 1C). The positive control, ionomycin, immediately increased cellular Ca^{2+} concentration and was then attenuated after around 30 min. Ca^{2+} influx initiated by GSK could be detected from 1 nM and increased dose-dependently.

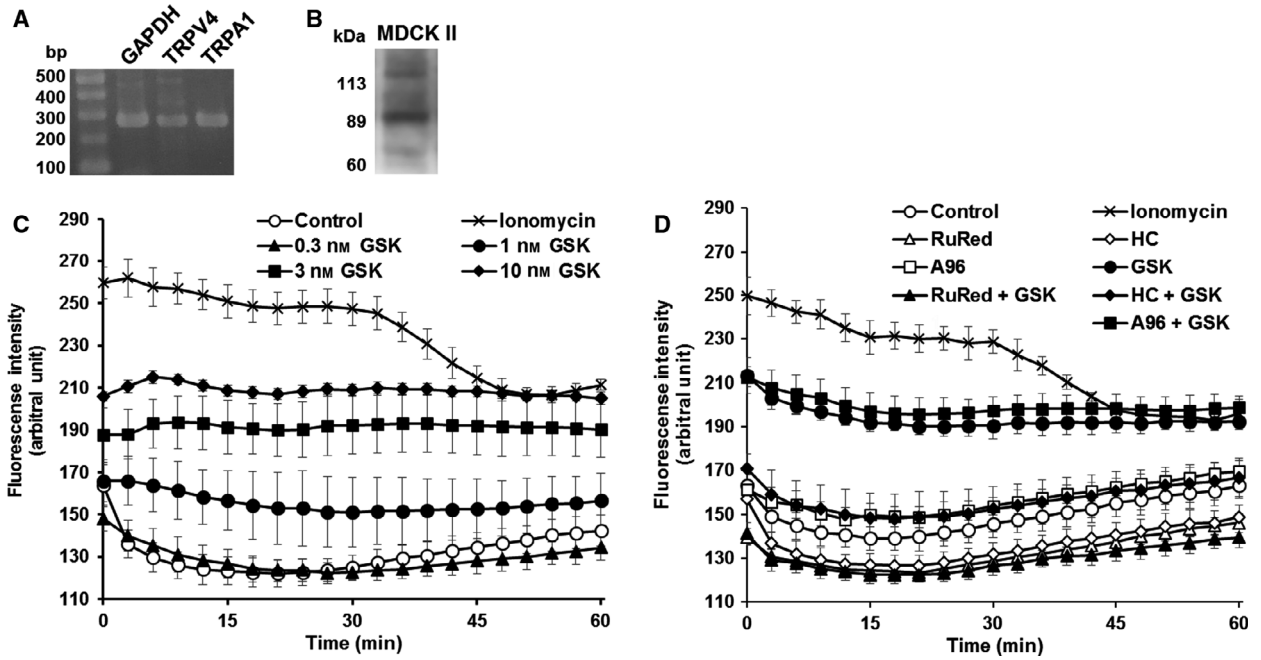

Fig. 1. Functional TRPV4 is expressed by MDCK II monolayers. (A) Expressions of TRPV4 and TRPA1 were confirmed by RT-PCR. Electrophoretic separation of PCR products produced with specific primers is shown. GAPDH was used as a control. Expected product sizes are as follows: GAPDH, 271 bp; TRPV4, 270 bp; and TRPA1, 272 bp. (B) TRPV4 protein expression was analyzed by immunoblotting using anti-TRPV4 antibody in MDCK II monolayer. (C) Several doses of GSK were employed to analyze Ca^{2+} influx in MDCK II monolayers. (○) DMSO control, (×) 10 μM ionomycin, (▲) 0.3 nM, (●) 1 nM, (■) 3 nM, and (◆) 10 nM GSK. Each value represents the mean ± standard deviation in triplicate experiments. (D) Cells were pretreated with TRPV4 antagonists (10 μM RuRed and 1 μM HC) and TRPA1 antagonist (1 μM A96) for 30 min prior to 1 nM GSK addition. (○) DMSO control, (×) 10 μM ionomycin, (Δ) 10 μM RuRed, (◇)1 μM HC, (□) 1 μM A96, (●) 1 nM GSK, (▲) 10 μM RuRed + 1 nM GSK, and (◆) 1 μM HC + 1 nM GSK, and (■) 1 μM A96 + 1 nM GSK. Each value represents the mean ± standard deviation in triplicate experiments.

To analyze the contribution of TRPV4 channels to the Ca^{2+} influx, we used ruthenium red (RuRed), which acts as a broad inhibitor of a wide range of cation channels, including TRPV family members, and a TRPV4-specific antagonist, HC-067047 (HC). One nanomolar GSK induced rapid and sustained Ca^{2+} influx that was completely blocked by 10 μM RuRed and 1 μM HC (Fig. 1D). These data demonstrate that MDCK II monolayers express functional TRPV4 ion channels.

The TRPV4 agonist GSK induces reversible TJ opening in MDCK II monolayers

Before investigating the effects of GSK on TJ function, we examined the cytotoxicity of GSK to MDCK II monolayers. The IC_{50} of GSK was determined to be 5.8 ± 1.2 nM, and GSK did not exhibit notable cytotoxicity at 1 nM after 5 h of exposure to the monolayers (Fig. S1).

We next examined whether or not GSK can increase TJ permeability. An FD4 solution was applied to the apical sides of MDCK II monolayers grown in transwells, which were then treated with different concentrations of GSK. Every 30 min, the basolateral solution was collected to quantify the amount of permeated FD4 (Fig. 2A,B). Latrunculin A (LatA), an irreversible TJ opener, increased FD4 permeability continuously [13]. As with LatA, 3 nM GSK continuously increased FD4 permeability from 30 min to 5 h, indicating an irreversible TJ opening. Note that in this figure, we use a logarithmic scale for the *Y*-axis (relative cumulative fluorescence intensity), because 3 nM GSK increased permeability much more than LatA. In contrast, 1 nM GSK induced reversible opening of TJs, which opened in as little as 15 min (Figs 2C,E and 3B, F) and then closed in around 2 h. A lower dose of GSK (0.3 nM) did not induce FD4 permeability. We therefore used 1 nM GSK for further experiments.

We previously reported that capsaicin and other natural α,β-unsaturated carbonyl compounds induce reversible opening of TJs *via* Ca^{2+} influx [11–13]. We therefore investigated TRPV4 involvement in GSK-induced reversible TJ opening and found that HC inhibited GSK-induced FD4 permeability completely

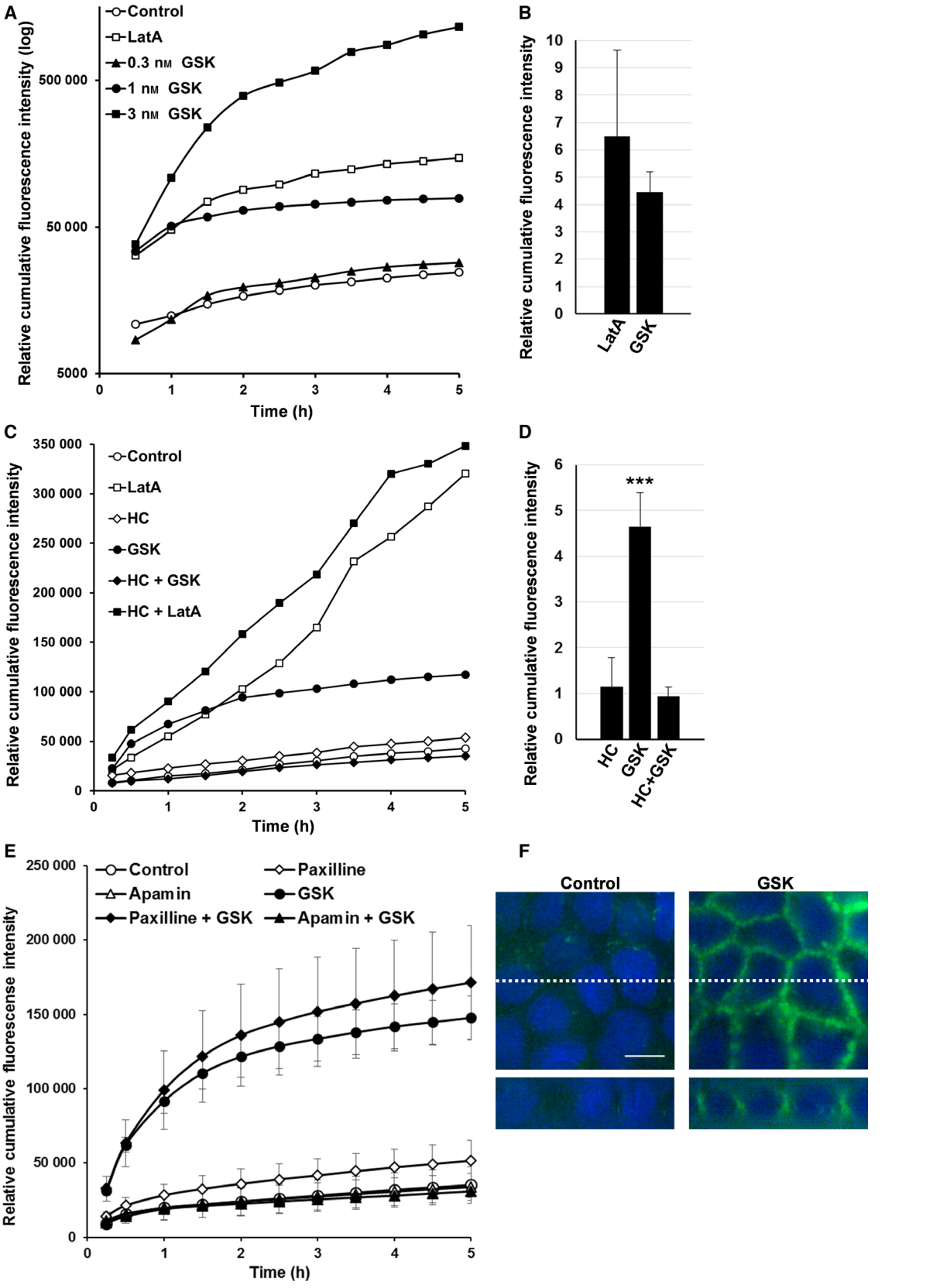
A
Control
LatA
0.3 nM GSK
1 nM GSK
3 nM GSK
Relative cumulative fluorescence intensity (log)
500 000
50 000
5000
0
1
2
3
4
5
Time (h)
B
Relative cumulative fluorescence intensity
10
9
8
7
6
5
4
3
2
1
0
LatA
GSK
C
Control
LatA
HC
GSK
HC + GSK
HC + LatA
Relative cumulative fluorescence intensity
350 000
300 000
250 000
200 000
150 000
100 000
50 000
0
Time (h)
D
Relative cumulative fluorescence intensity
***
6
5
4
3
2
1
0
HC
GSK
HC+GSK
E
Control
Paxilline
Apamin
GSK
Paxilline + GSK
Apamin + GSK
Relative cumulative fluorescense intensity
250 000
200 000
150 000
100 000
50 000
0
Time (h)
F
Control
GSK

Fig. 2. GSK reversibly increases the paracellular permeability of MDCK II monolayers. (A) GSK modulated the epithelial permeability of MDCK II monolayer. Three nanomolar GSK induced an irreversible FD4 permeability increase, 1 nM GSK reversibly increased permeability, and 0.3 nM GSK did not. (○) DMSO control, (□) 0.1 μM LatA, and (▲) 0.3 nM, (●) 1 nM, and (◆) 3 nM GSK. Typical data of three independent experiments is shown. (B) The efficiencies of TJ permeability enhancement induced by 0.1 μM LatA and 1 nM GSK were evaluated by the cumulative FD4 amounts transported until 2 h relative to the vehicle control. Each value represents the mean ± standard deviation of three independent experiments. (C) The specific TRPV4 antagonist 1 μM HC abolished the FD4 permeability increase induced by 1 nM GSK. (○) DMSO control, (□) 0.1 μM LatA, (◇) 1 μM HC, (●) 1 nM GSK, (◆) 1 μM HC + 1 nM GSK, and (■) 1 μM HC + 0.1 μM LatA. Typical data of three independent experiments is shown. (D) The inhibitory effect of HC on the TJ permeability enhancement induced by GSK was evaluated by comparing the cumulative FD4 amounts transported by 1 μM HC, 1 nM GSK, and 1 μM HC + 1 nM GSK until 2 h relative to the vehicle control. Each value represents the mean ± standard deviation of four independent experiments. *** indicate that the value is significantly ($P < 0.001$) different from others. (E) The SK channel blocker apamin (1 μM), but not the BK channel blocker paxilline (30 μM), inhibit the FD4 permeability increase induced by 1 nM GSK. (○) DMSO control, (□) 0.1 μM LatA, (◇) 30 μM paxilline, (Δ) 1 μM apamin, (●) 1 nM GSK, (◆) 30 μM paxilline + 1 nM GSK, and (▲) 1 μM apamin + 1 nM GSK. Each value represents the mean ± standard deviation in triplicate experiments. (F) Deconvoluted images of MDCK II monolayers after 30 min incubation with (left) 1% FD4 and DMSO, (right) 1% FD4 and 1 nM GSK. Top: XY sections of merged images. Bottom: XZ sections of merged images. Top is apical, bottom is basolateral. Scale bar: 10 μm.

(Fig. 2C,D), suggesting that the TJ permeability increase induced by GSK is mediated by TRPV4. HC did not affect LatA-induced permeability increase at all under the same conditions, because LatA opens TJs irreversibly by depolymerizing actin filaments.

It has been reported that Ca^{2+} entry *via* TRPV4 upon 4α-phorbol 12,13-didecanoate (4α-PDD) stimulation activates large conductance Ca^{2+}-activated K^+ channels (BK channels) in a mouse mammary cell line, resulting in an increase in transcellular/paracellular permeability for at least until 24 h [7]. Because BK channels are expressed in kidney epithelial cells [22], there is a possibility that TJ opening is correlated with the activation of BK channels. We therefore investigated the involvement of BK channels in GSK-induced TJ opening. The specific BK channel blocker, paxilline, did not block both GSK-induced FD4 permeability (Fig. 2E) and TER decrease (Fig. S2), suggesting that BK channels are not involved in GSK-induced TJ opening.

On the other hand, there is a report that TRPV4-mediated Ca^{2+} influx activates small conductance Ca^{2+}-activated K^+ channels (SK channels) in renal collecting duct cells [23]. When we employed SK channel inhibitor apamin to the GSK-induced FD4 permeability experiment, it blunted the permeability increase (Fig. 2E). Taken together, not BK but SK channels are suggested to be involved in GSK-induced TJ opening.

Finally, transport of FD4 across the MDCK II monolayer was demonstrated using fluorescent microscopy as described in Materials and methods. Images were taken after incubation of the monolayers with FD4 with or without GSK, as shown in Fig. 2F. In control monolayers, the uptake of fluorescent was not generally observed. Addition of GSK resulted in increased paracellular uptake of fluorescence.

Mechanistic comparison with capsaicin TJ opening *via* TRPA1

We next analyzed the mechanisms underlying the GSK-induced reversible opening of TJs. We have previously shown that Ca^{2+} entry triggers capsaicin-induced TJ opening [11,12]; therefore, we first confirmed whether this is also the case with GSK-induced TJ opening. To obtain direct evidence for a Ca^{2+} influx requirement for GSK-induced reversible TJ opening, we removed Ca^{2+} from the assay buffer (Materials and methods). Because Ca^{2+} depletion itself gradually opens TJs [11,24–27], we measured TER and FD4 permeability for 30 min. GSK induced a considerable decrease in TER within 5 min in the presence of Ca^{2+} (Fig. 3A), whereas the DMSO control did not. In contrast, GSK did not lead to any decrease in TER in the absence of Ca^{2+}, which was the same as DMSO control until 10 min. After 15 min, GSK decreased TER gradually, but so did the DMSO control, suggesting that this TER decrease was caused by Ca^{2+} depletion. Consistent with this result, the increase in FD4 permeability induced by GSK was also abolished in the absence of Ca^{2+} (Fig. 3B), although Ca^{2+} depletion itself was relatively less affective. Taken together, these results suggest that Ca^{2+} entry is necessary to induce reversible TJ opening by GSK, similarly to what is observed with capsaicin.

Next, we focused on cofilin dephosphoryaltion (activation), which is a critical signal for capsaicin-induced TJ opening [11,12]. We have shown that almost all cofilin is dephosphorylated as quickly as 10 min and then rephosphorylated at around 60 min upon capsaicin treatment. Because GSK induced a rapid increase in TJ permeability within 10 min (Fig. 3A,B), we analyzed changes in cofilin phosphorylation within

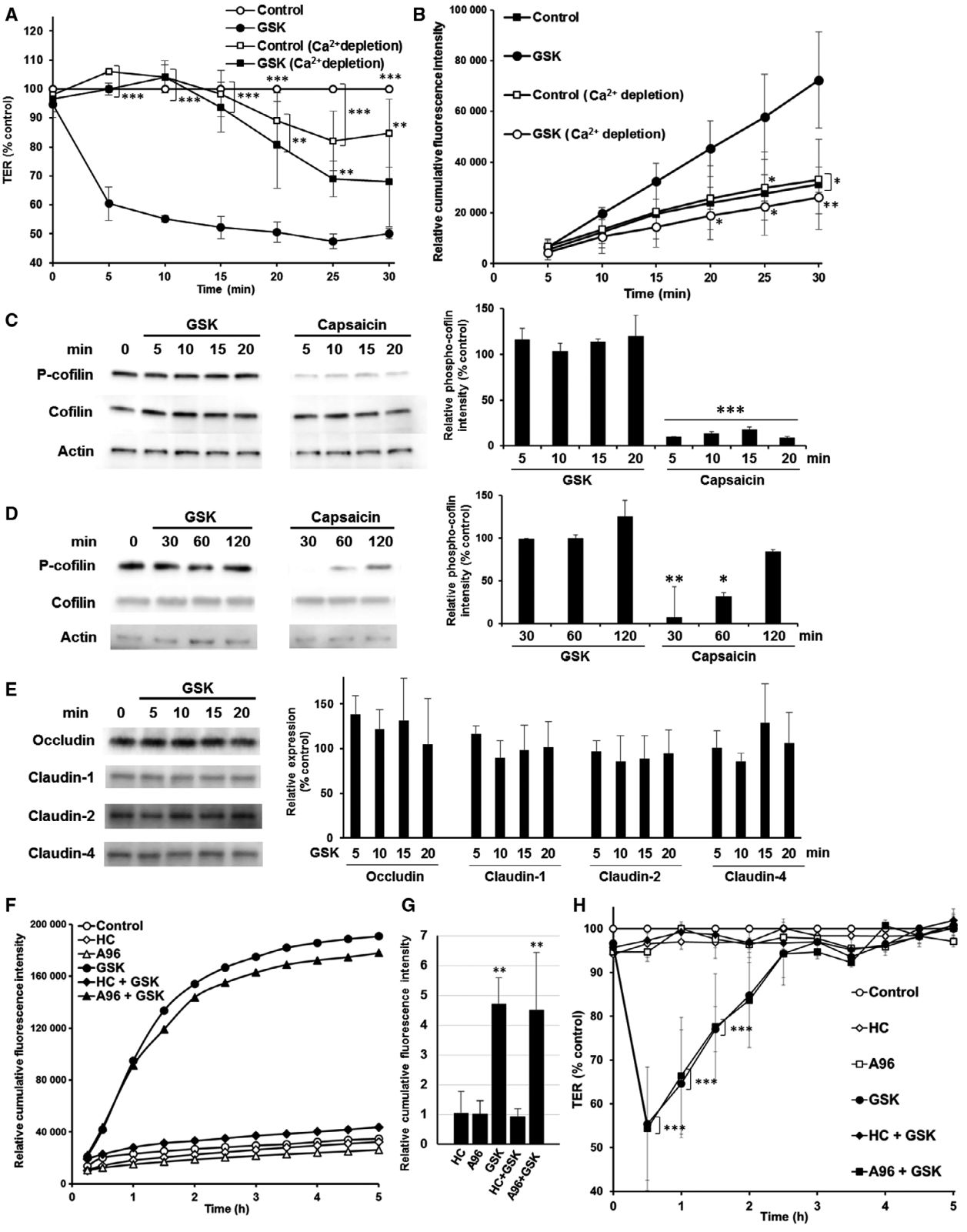
A
Control
GSK
Control (Ca2+depletion)
GSK (Ca2+depletion)
TER (% control)
Time (min)
B
Control
GSK
Control (Ca2+ depletion)
GSK (Ca2+ depletion)
Relative cumulative fluorescence intensity
Time (min)
C
GSK
Capsaicin
min
P-cofilin
Cofilin
Actin
Relative phospho-cofilin intensity (% control)
GSK
Capsaicin
D
GSK
Capsaicin
min
P-cofilin
Cofilin
Actin
Relative phospho-cofilin intensity (% control)
GSK
Capsaicin
E
GSK
min
Occludin
Claudin-1
Claudin-2
Claudin-4
Relative expression (% control)
GSK
Occludin
Claudin-1
Claudin-2
Claudin-4
F
Control
HC
A96
GSK
HC + GSK
A96 + GSK
Relative cumulative fluorescence intensity
Time (h)
G
Relative cumulative fluorescence intensity
HC
A96
GSK
HC+GSK
A96+GSK
H
Control
HC
A96
GSK
HC + GSK
A96 + GSK
TER (% control)
Time (h)

Fig. 3. Ca^{2+} influx, but not cofilin and TRPA1, is involved in GSK-induced modulation of MDCK II epithelia. (A, B) Ca^{2+} depletion blocks the GSK-induced TER decrease (A) and FD4 permeability increase (B). MDCK II monolayers were treated with 1 nM GSK, with or without 1.3 mM Ca^{2+}. Changes in TER and amounts of permeated FD4 were analyzed at each time point. Each value represents the mean ± standard deviation of three independent experiments. (○) DMSO control, (●) 1 nM GSK, (□) DMSO control under Ca^{2+}-depleted conditions, (■) 1 nM GSK under Ca^{2+}-depleted conditions. Dunnett's test has been performed comparing with GSK treatment at each time. $*P < 0.05$; $**P < 0.01$; $***P < 0.001$. (C, D) GSK did not induce a notable change in the phosphorylation of cofilin protein. MDCK II monolayers were treated with 1 nM GSK or 300 μM capsaicin for the indicated durations. Representative data from three independent western blot analyses of phosphorylated cofilin, cofilin, and actin are shown. The bar shows a densitometric analysis of phosphorylated cofilin. The band intensity at each time point is relative to that of time 0 and is shown as the mean ± standard deviation of three independent experiments. Dunnett's test has been performed comparing each treatment with time 0 control. $*P < 0.05$; $**P < 0.01$; $***P < 0.001$. (E) GSK did not induce notable changes in the expression of occludin and claudin-1, -2, -4 proteins. MDCK II monolayers were treated with 1 nM GSK for the indicated durations. Representative data from three independent western blot analyses are shown. The bar shows the densitometric analysis of each protein expression. The band intensity at each time point is relative to that of time 0 and is shown as the mean ± standard deviation of three independent experiments. Dunnett's test has been performed comparing each treatment with time 0 control, and found to be not significant. (F, H) TRPV4 antagonist (1 μM HC) pretreatment for 30 min inhibited the GSK-induced FD4 permeability increase (F) and TER decrease (H), but a TRPA1 antagonist (1 μM A96) did not. (○) DMSO control, (◇) 1 μM HC, (△) 1 μM A96, (●) 1 nM GSK, (◆) 1 μM HC + 1 nM GSK, and (▲) 1 μM A96 + 1 nM GSK. Typical data of three independent experiments is shown (F), or each value represents the mean ± standard deviation of three independent experiments (H). In (H), Dunnett's test has been performed comparing with vehicle control at each time. $***P < 0.001$. (G) The inhibitory effect of HC and no influence of A96 on the TJ permeability enhancement induced by GSK was evaluated by comparing the cumulative FD4 amounts transported by 1 μM HC, 1 μM A96, 1 nM GSK, 1 μM HC + 1 nM GSK and 1 μM A96 + 1 nM GSK until 2 h relative to the vehicle control. Each value represents the mean ± standard deviation of three independent experiments. Dunnett's test has been performed comparing with the control. $**P < 0.01$.

the first 20 min of treatment (Fig. 3C, left). Capsaicin induced a significant decrease in cofilin phosphorylation as quickly as 5 min, and this persisted over 20 min. In contrast, GSK did not produce such a decrease even though it should have already induced TJ opening by this time. These observations were confirmed by densitometric analysis (Fig. 3C, right). The same results were obtained in longer incubations up to 120 min. Consistent with our previous report, cofilin phosphorylation recovered after 60 min of capsaicin treatment, although GSK did not induce any notable change in its phosphorylation level (Fig. 3D). These results suggest that although both GSK and capsaicin require a Ca^{2+} influx to trigger TJ opening, the resulting downstream signaling appears to be different. In addition, we also analyzed the expression of occludin, claudin-1, -2, -4, as they are the main regulator of TJ, however, there were no significant change (Fig. 3E). Furthermore, we also examined the distributions of occludin and claudin-1 by immunofluorescence, but could not observe marked difference between control and GSK treatment (Fig. S3).

It is possible that TRPV4 activation by GSK might induce TJ opening *via* TRPA1 sensitization/activation [28–31]. We therefore examined the involvement of TRPA1 in GSK-induced TJ opening pathways to further elucidate the difference in mechanisms between GSK and capsaicin. The Ca^{2+} influx induced by GSK was unaffected by the TRPA1 antagonist A-967079 (A96; Fig. 1D). We confirmed that the TRPA1 agonist AITC also induced Ca^{2+} influx, which was blocked by A96, but not by HC under the same conditions (Fig. S4). The ineffectiveness of the TRPA1 antagonist at inhibiting the GSK-induced epithelial permeability increase was confirmed by both the FD4 permeability (Fig. 3F,G) and TER experiments (Fig. 3H). These results suggest that, although sharing necessity of a Ca^{2+} influx, GSK opens TJs *via* a different channel and downstream mechanism than capsaicin.

Discussion

In the present study, we evaluated TRPV4 expression and involvement in the reversible opening of TJs in MDCK II epithelial monolayers. The TRPV4 agonist GSK increased intracellular Ca^{2+} in MDCK II monolayer, and the responses were significantly inhibited by the specific TRPV4 agonist HC, but not by the TRPA1 antagonist A96. These results indicate that TRPV4 is functionally expressed in MDCK II monolayers.

GSK induced a reversible paracellular permeability increase and TER decrease at nontoxic concentrations, suggesting that the TJ opening was reversible. The GSK-induced TJ opening was potently inhibited by the TRPV4 antagonist (HC), but not by paxilline. GSK-induced TER decreases eventually returned to basal levels, suggesting that cell viability was normal. Because it has been reported that TRPV4 activation is associated with a rapid downregulation of TRPV4 at the plasma membrane, leading to rapid desensitization [32,33], GSK stimulation on TRPV4 might be temporary, resulting in reversible effects.

TRPV4 activation increases epithelial permeability in the mouse mammary cell line HC11, and this is prevented by the BK channel blocker paxilline in the early phase [7]. We have not demonstrated the expression of BK channels in MDCK II cells, but they are known to be expressed in epithelial cells of the kidney and in C11-MDCK cells [22,34]. However, we observed no inhibition of GSK-induced TJ opening by paxilline. This observation, together with a report that the permeability increase is not reversed until at least 24 h in 4α-PDD-stimulated HC11 cells [7], suggests that the processes and the resulting effects including reversibility of the epithelial permeability increase, and the underlying mechanisms are different from what we revealed here. Instead, here we found that SK channels are involved in GSK-induced TJ opening. We are now analyzing the interplay between TRPV4 and SK channels and the downstream mechanism. On the other hand, several reports have shown that TRPV4 activation strengthens epithelial TJs [4–10], and we are currently investigating the basis of these differences, including TJ protein modulation.

We have been analyzing the reagents that induce the reversible opening of TJs, for example, capsaicin and natural compounds containing an α,β-unsaturated moiety, and have discovered that a specific cofilin dephosphorylation and F-actin modulation are important for TJ opening to be reversible [13,17]. Here, we observed the highly reproducible and complete reversal in TRPV4-mediated TJ opening. We primarily expected that the TJ opening mechanism of GSK would be the same as capsaicin's, that is, that GSK action would also involve Ca^{2+} influx and cofilin-actin modulation, because these two compounds induced a similar reversible pattern of TJ opening triggered by Ca^{2+} influx in MDCK II monolayers. However, GSK did not activate cofilin even though Ca^{2+} influx is involved early in the opening of TJ by both capsaicin and GSK. Because capsaicin and GSK activate different channels, i.e., TRPA1 for capsaicin and TRPV4 for GSK, these results suggest that the Ca^{2+} increase induced by the stimulation of different TRP channels recruits different molecules and/or transmits different signals for barrier regulation.

The MDCK cell line was isolated from the kidney cortex [35], and high expression of TRPV4 has been shown in the kidney [19]. There are several reports of TRPV4 expression in the nephron segment in kidney. One showed that water-impermeant tubular segments, such as the thick ascending limb and the distal convoluted tubule, express abundant TRPV4, suggesting an osmoregulatory role for TRPV4 in these nephron segments where an osmotic gradient is generated [36]. Subsequent studies have reported that TRPV4 is expressed in several tubule segments, and collecting ducts, where it appears to function as a flow sensor inducing a rapid influx of Ca^{2+} [37,38]. Consistently, it has also been reported that TRPV4 is an essential component of the ciliary flow sensor and is associated with transient Ca^{2+} influx in MDCK cells [39]. Since TRPV4 responds to osmotic cell swelling and flow-induced mechanical stress, leading to an influx of Ca^{2+} [23,40], and since we observed that Ca^{2+} influx is responsible for the reversible opening of TJs (Fig. 3A), TRPV4-mediated TJ regulation may function to adjust to changes in extracellular osmolarity and/or flow rate under physiological conditions.

In conclusion, we have shown that TRPV4 activation induces Ca^{2+} influx, resulting in the reversible opening of TJs. An analysis of the mechanism underlying this opening, and its physiological role, is underway.

Acknowledgments

This work was supported by grants from Japan Society for Bioscience, Biotechnology, and Agrochemistry to TU (JSBBA Innovative Research Program Award), and the Center of Innovation Program funded by the Ministry of Education Culture and Sports (MEXT), Japan and Japan Science and Technology (JST) to YN. The authors thank Enago (www.enago.jp) for the English language review.

Author contributions

MM and YY performed the experiments, analysis, and interpretation of data. TU and YN contributed to the conception and design of the study, analysis and interpretation of data, and writing of the manuscript.

References

1 Thorneloe KS, Sulpizio AC, Lin Z, Figueroa DJ, Clouse AK, McCafferty GP, Chendrimada TP, Lashinger ES, Gordon E, Evans L *et al.* (2008) N-((1S)-1-{[4-((2S)-2-{[(2,4-dichlorophenyl)sulfonyl]amino}-3-hydroxypropanoyl)-1-piperazinyl]carbonyl}-3-methylbutyl)-1-benzothiophene-2-carboxamide (GSK1016790A), a novel and potent transient receptor potential vanilloid 4 channel agonist induces urinary bladder contraction and hyperactivity: part I. *J Pharmacol Exp Ther* **326**, 432–442.

2 Wu S, Jian MY, Xu YC, Zhou C, Al-Mehdi AB, Liedtke W, Shin HS and Townsley MI (2009) Ca2+ entry via alpha1G and TRPV4 channels differentially

regulates surface expression of P-selectin and barrier integrity in pulmonary capillary endothelium. *Am J Physiol Lung Cell Mol Physiol* **297**, L650–L657.
3 Cioffi DL, Lowe K, Alvarez DF, Barry C and Stevens T (2009) TRPing on the lung endothelium: calcium channels that regulate barrier function. *Antioxid Redox Signal* **11**, 765–776.
4 Akazawa Y, Yuki T, Yoshida H, Sugiyama Y and Inoue S (2013) Activation of TRPV4 strengthens the tight-junction barrier in human epidermal keratinocytes. *Skin Pharmacol Physiol* **26**, 15–21.
5 Kida N, Sokabe T, Kashio M, Haruna K, Mizuno Y, Suga Y, Nishikawa K, Kanamaru A, Hongo M, Oba A *et al.* (2012) Importance of transient receptor potential vanilloid 4 (TRPV4) in epidermal barrier function in human skin keratinocytes. *Pflugers Arch* **463**, 715–725.
6 Martinez-Rendon J, Sanchez-Guzman E, Rueda A, Gonzalez J, Gulias-Canizo R, Aquino-Jarquin G, Castro-Munozledo F and Garcia-Villegas R (2017) TRPV4 regulates tight junctions and affects differentiation in a cell culture model of the corneal epithelium. *J Cell Physiol* **232**, 1794–1807.
7 Reiter B, Kraft R, Gunzel D, Zeissig S, Schulzke JD, Fromm M and Harteneck C (2006) TRPV4-mediated regulation of epithelial permeability. *FASEB J* **20**, 1802–1812.
8 Sokabe T, Fukumi-Tominaga T, Yonemura S, Mizuno A and Tominaga M (2010) The TRPV4 channel contributes to intercellular junction formation in keratinocytes. *J Biol Chem* **285**, 18749–18758.
9 Sokabe T and Tominaga M (2010) The TRPV4 cation channel: a molecule linking skin temperature and barrier function. *Commun Integr Biol* **3**, 619–621.
10 Yamawaki H, Mihara H, Suzuki N, Nishizono H, Uchida K, Watanabe S, Tominaga M and Sugiyama T (2014) Role of transient receptor potential vanilloid 4 activation in indomethacin-induced intestinal damage. *Am J Physiol Gastrointest Liver Physiol* **307**, G33–G40.
11 Nagumo Y, Han J, Arimoto M, Isoda H and Tanaka T (2007) Capsaicin induces cofilin dephosphorylation in human intestinal cells: the triggering role of cofilin in tight-junction signaling. *Biochem Biophys Res Commun* **355**, 520–525.
12 Nagumo Y, Han J, Bellila A, Isoda H and Tanaka T (2008) Cofilin mediates tight-junction opening by redistributing actin and tight-junction proteins. *Biochem Biophys Res Commun* **377**, 921–925.
13 Shiobara T, Usui T, Han J, Isoda H and Nagumo Y (2013) The reversible increase in tight junction permeability induced by capsaicin is mediated via cofilin-actin cytoskeletal dynamics and decreased level of occludin. *PLoS One* **8**, e79954.
14 Han JK, Isoda H and Maekawa T (2002) Analysis of the mechanism of the tight-junctional permeability increase by capsaicin treatment on the intestinal caco-2 cells. *Cytotechnology* **40**, 93–98.
15 Han JK, Akutsu M, Talorete TPN, Maekawa T, Tanaka T and Isoda H (2005) Capsaicin-enhanced ribosomal protein P2 expression in human intestinal caco-2 cells. *Cytotechnology* **47**, 89–96.
16 Isoda H, Han JK, Tominaga M and Maekawa T (2001) Effect of capsaicin on human intestinal cell line caco-2. *Cytotechnology* **36**, 155–161.
17 Kanda Y, Yamasaki Y, Sasaki-Yamaguchi Y, Ida-Koga N, Kamisuki S, Sugawara F, Nagumo Y and Usui T (2018) TRPA1-dependent reversible opening of tight junction by natural compounds with an alpha, beta-unsaturated moiety and capsaicin. *Sci Rep* **8**, 2251.
18 Everaerts W, Zhen X, Ghosh D, Vriens J, Gevaert T, Gilbert JP, Hayward NJ, McNamara CR, Xue F, Moran MM *et al.* (2010) Inhibition of the cation channel TRPV4 improves bladder function in mice and rats with cyclophosphamide-induced cystitis. *Proc Natl Acad Sci USA* **107**, 19084–19089.
19 Strotmann R, Harteneck C, Nunnenmacher K, Schultz G and Plant TD (2000) OTRPC4, a nonselective cation channel that confers sensitivity to extracellular osmolarity. *Nat Cell Biol* **2**, 695–702.
20 Ning JZ, Li W, Cheng F, Yu WM, Rao T, Ruan Y, Yuan R, Zhang XB, Zhuo D, Du Y *et al.* (2017) MiR-29a suppresses spermatogenic cell apoptosis in testicular ischemia-reperfusion injury by targeting TRPV4 channels. *Front Physiol* **8**, 966.
21 Zaika O, Mamenko M, Berrout J, Boukelmoune N, O'Neil RG and Pochynyuk O (2013) TRPV4 dysfunction promotes renal cystogenesis in autosomal recessive polycystic kidney disease. *J Am Soc Nephrol* **24**, 604–616.
22 Gonzalez-Perez V and Lingle CJ (2019) Regulation of BK channels by beta and gamma subunits. *Annu Rev Physiol* **81**, 113–137.
23 Jin M, Berrout J, Chen L and O'Neil RG (2012) Hypotonicity-induced TRPV4 function in renal collecting duct cells: modulation by progressive cross-talk with Ca2 + -activated K + channels. *Cell Calcium* **51**, 131–139.
24 Stevenson BR and Begg DA (1994) Concentration-dependent effects of cytochalasin D on tight junctions and actin filaments in MDCK epithelial cells. *J Cell Sci* **107** (Pt 3), 367–375.
25 Martinez-Palomo A, Meza I, Beaty G and Cereijido M (1980) Experimental modulation of occluding junctions in a cultured transporting epithelium. *J Cell Biol* **87**, 736–745.
26 Ma TY, Tran D, Hoa N, Nguyen D, Merryfield M and Tarnawski A (2000) Mechanism of extracellular calcium regulation of intestinal epithelial tight junction permeability: role of cytoskeletal involvement. *Microsc Res Tech* **51**, 156–168.

27 Ivanov AI, McCall IC, Parkos CA and Nusrat A (2004) Role for actin filament turnover and a myosin II motor in cytoskeleton-driven disassembly of the epithelial apical junctional complex. *Mol Biol Cell* **15**, 2639–2651.
28 Marko L, Mannaa M, Haschler TN, Kramer S and Gollasch M (2017) Renoprotection: focus on TRPV1, TRPV4, TRPC6 and TRPM2. *Acta Physiol (Oxf)* **219**, 589–612.
29 Zhang ZR, Chu WF, Song B, Gooz M, Zhang JN, Yu CJ, Jiang S, Baldys A, Gooz P, Steele S *et al.* (2013) TRPP2 and TRPV4 form an EGF-activated calcium permeable channel at the apical membrane of renal collecting duct cells. *PLoS One* **8**, e73424.
30 Akopian AN, Ruparel NB, Jeske NA and Hargreaves KM (2007) Transient receptor potential TRPA1 channel desensitization in sensory neurons is agonist dependent and regulated by TRPV1-directed internalization. *J Physiol* **583**, 175–193.
31 Spahn V, Stein C and Zollner C (2014) Modulation of transient receptor vanilloid 1 activity by transient receptor potential ankyrin 1. *Mol Pharmacol* **85**, 335–344.
32 Jin M, Wu Z, Chen L, Jaimes J, Collins D, Walters ET and O'Neil RG (2011) Determinants of TRPV4 activity following selective activation by small molecule agonist GSK1016790A. *PLoS One* **6**, e16713.
33 Shukla AK, Kim J, Ahn S, Xiao K, Shenoy SK, Liedtke W and Lefkowitz RJ (2010) Arresting a transient receptor potential (TRP) channel: beta-arrestin 1 mediates ubiquitination and functional down-regulation of TRPV4. *J Biol Chem* **285**, 30115–30125.
34 Holtzclaw JD, Liu L, Grimm PR and Sansom SC (2010) Shear stress-induced volume decrease in C11-MDCK cells by BK-alpha/beta4. *Am J Physiol Renal Physiol* **299**, F507–F516.
35 Herzlinger DA, Easton TG and Ojakian GK (1982) The MDCK epithelial cell line expresses a cell surface antigen of the kidney distal tubule. *J Cell Biol* **93**, 269–277.
36 Tian W, Salanova M, Xu H, Lindsley JN, Oyama TT, Anderson S, Bachmann S and Cohen DM (2004) Renal expression of osmotically responsive cation channel TRPV4 is restricted to water-impermeant nephron segments. *Am J Physiol Renal Physiol* **287**, F17–F24.
37 Berrout J, Jin M, Mamenko M, Zaika O, Pochynyuk O and O'Neil RG (2012) Function of transient receptor potential cation channel subfamily V member 4 (TRPV4) as a mechanical transducer in flow-sensitive segments of renal collecting duct system. *J Biol Chem* **287**, 8782–8791.
38 Janas S, Seghers F, Schakman O, Alsady M, Deen P, Vriens J, Tissir F, Nilius B, Loffing J, Gailly P *et al.* (2016) TRPV4 is associated with central rather than nephrogenic osmoregulation. *Pflugers Arch* **468**, 1595–1607.
39 Kottgen M, Buchholz B, Garcia-Gonzalez MA, Kotsis F, Fu X, Doerken M, Boehlke C, Steffl D, Tauber R, Wegierski T *et al.* (2008) TRPP2 and TRPV4 form a polymodal sensory channel complex. *J Cell Biol* **182**, 437–447.
40 Cabral PD, Capurro C and Garvin JL (2015) TRPV4 mediates flow-induced increases in intracellular ca in medullary thick ascending limbs. *Acta Physiol (Oxf)* **214**, 319–328.

Supporting information

Additional supporting information may be found online in the Supporting Information section at the end of the article.

Fig. S1. GSK cytotoxicity to MDCK II monolayers.

Fig. S2. BK channel is not involved in GSK-induced TJ opening.

Fig. S3. Distribution of occludin and claudin-1 in GSK-treated cells.

Fig. S4. The Ca^{2+} influx induced by the TRPA1 agonist AITC is blocked by A96, but not by HC.